Green Chemistry

Controlling the toxicity of biomass-derived difunctional molecules as potential pharmaceutical ingredients for specific activity toward microorganisms and mammalian cells

Journal:	*Green Chemistry*
Manuscript ID	GC-ART-01-2023-000188.R2
Article Type:	Paper
Date Submitted by the Author:	25-Mar-2023

Complete List of Authors:	Chang, Hochan; University of Wisconsin Madison, Chemical and Biological Engineering Chang, Douglas ; University of Wisconsin-Madison, Chemical and Biological Engineering Stamoulis, Alexios; University of Wisconsin-Madison, Chemistry Huber, George; University of Wisconsin, Chemical and Biological Engineering Lynn, David; University of Wisconsin-Madison, Chemical and Biological Engineering; University of Wisconsin-Madison, Chemistry Palecek, Sean; University of Wisconsin-Madison, Chemical and biological engineering Dumesic, James; University of Wisconsin Madison, Chemical and Biological Engineering

ARTICLE

Controlling the toxicity of biomass-derived difunctional molecules as potential pharmaceutical ingredients for specific activity toward microorganisms and mammalian cells

Received 00th January 20xx,
Accepted 00th January 20xx

DOI: 10.1039/x0xx00000x

Hochan Chang[‡a], Douglas H. Chang[‡a], Alexios G. Stamoulis[b], George W. Huber[a], David M. Lynn[a,b], Sean P. Palecek[a], James A. Dumesic[a,c]*

A biomass-derived difuran compound, denoted as HAH (HMF-Acetone-HMF), synthesized by aldol-condensation of 5-hydroxyfurfural (HMF) and acetone, can be partially hydrogenated to provide an electron-rich difuran compound (PHAH) for Diels-Alder reactions with maleimide derivatives. The nitrogen (N) site in the maleimide can be substituted by imidation with amine-containing compounds to control the hydrophobicity of the maleimide moiety in adducts of furans and maleimide by Diels-Alder reaction, denoted as norcantharimides (Diels-Alder adducts). The structural effects on the toxicity of various biomass-derived small molecules synthesized in this manner to regulate biological processes, defined as low molecular weight (≤ 1000 g/mol) organic compounds, were investigated against diverse microbial and mammalian cell types. The biological toxicity increased when hydrophobic N-substitutions and C=C bonds were introduced into the molecular structure. Among the synthesized norcantharamide derivatives, some compounds demonstrated pH-dependent toxicities against specific cell types. Reaction kinetics analyses of the norcantharimides in biological conditions suggest that this pH-dependent toxicity of norcantharimides could arise from retro Diels-Alder reactions in the presence of a Brϕnsted acid that catalyzes the release of an N-substituted maleimide, which has higher toxicity against fungal cells than the toxicity of the Diels-Alder adduct. These synthetic approaches can be used to design biologically-active small molecules that exhibit selective toxicity against various cell types (e.g., fungal, cancer cells) and provide a sustainable platform for production of prodrugs that could actively or passively affect the viability of infectious cells.

1. Introduction

Biomass-derived compounds provide a source for furan derivatives that can be activated for Diels-Alder reactions[1], which is a click-chemistry reaction for the production of unique reversible linkages at room temperature.[2] This linkage can be cleaved by a retro Diels-Alder reaction at moderately elevated temperatures (≥60℃).[3] Diels-Alder reactions have the potential to provide a powerful tool for the design of drug delivery systems and biomaterials.[2] For instance, furan-containing polymeric resins have been reported for the production of self-healing materials[4], drug delivery cargos, and dynamic material fabrication as biomedical applications.[5]

Diels-Alder adducts, such as cantharidins, norcantharidins, and norcantharimides have been previously reported to have therapeutic potential.[6,7] Diels-Alder reaction of furan derivatives and maleic anhydride produces norcantharidins (Scheme 1a),[8] which are naturally bioactive compounds found in blister beetles.[9] Imidation of maleic anhydride with amines can produce N-substituted maleimides[10] which show potential therapeutic activities.[11,12] Then, norcantharimides can be synthesized by Diels-Alder reaction of furans and the N-substituted maleimides (Scheme 1b).[13] Moreover, N-substitutions of the norcantharimides can be used to tailor their anticancer toxicities[14] or elucidate important interactions against COVID-19 targets.[15] Thus, synthesis of norcanthardrins and/or norcantharimides from biomass-derived furans can open new horizons to sustainably produce therapeutic small molecules for potential pharmaceutical applications. Since maleimide derivatives can become pharmaceutical ingredients[12], control of retro Diels-Alder reactions can be leveraged to deliver therapeutic maleimides to target locations using the furan derivatives as cargo compounds.[16] In addition, retro Diels-Alder reactions become dominant over the forward Diels-Alder reaction either at elevated temperatures (≥100℃)[17] or in the presence of Brϕnsted acids.[18,19] It is possible to take advantages of the pH-dependent reaction equilibrium for pH-responsive applications. For example, the pH distribution in human tumors is acidic in the core as the volume of tumor increases.[20] Therefore, furan derivatives can potentially carry maleimide-based therapeutic ingredients by Diels-Alder reaction to tumor cells or infection sites, and the lower pH of the infected tissues can catalyze the retro Diels-Alder reaction to release the maleimide-based drugs at physiological temperatures.

[a] Department of Chemical and Biological Engineering, University of Wisconsin–Madison, Madison, WI, USA.
[b] Department of Chemistry, University of Wisconsin–Madison, Madison, WI, USA.
[c] DOE Great Lakes Bioenergy Research Center, University of Wisconsin–Madison, Madison, WI, USA.
‡These authors contributed equally.
*Corresponding author. E-mail: jdumesic@wisc.edu
Electronic Supplementary Information (ESI) available: Separated word document. See DOI: 10.1039/x0xx00000x

Recently, anticancer activities of difunctional norcantharimides have been reported, and the molecular structure of the norcantharimides, such as difunctionality, has been shown to affect their anticancer activities.[21] This behavior implies that the production of difunctional norcantharimides can introduce unique biological applications, where the difunctionalities can be obtained by Diels-Alder reaction of difurans with diverse N-substituted maleimides. A difuran molecule has been synthesized by aldol-condensation of biomass-derived 5-hydroxymethyl furfural (HMF)[22] and acetone (Scheme 1c).[23] This biomass-derived difuran, denoted as HAH (H and A represent HMF and acetone, respectively), was partially hydrogenated over a Cu/γ-Al_2O_3 catalyst (Scheme 1c).[24,25] Each furan in the partially hydrogenated HAH complex (PHAH) possessed electron-rich properties, which enables Diels-Alder reaction with electron-deficient dienophiles, like maleimide compounds (Scheme 1d).[26] Fundamental understanding of the reaction kinetics and the thermodynamic equilibrium for retro Diels-Alder reactions of these difunctional Diels-Alder adducts are important to control the release of N-substituted maleimides for biological applications. There have been recent reaction kinetics analyses for retro Diels-Alder reactions of monofunctional Diel-Alder adducts.[17] However, reaction kinetics analyses for retro Diels-Alder reactions and biological applications of difunctional Diels-Alder adducts have not been demonstrated yet.

Herein, we examined the toxicity of biomass-derived difuran (HAH), its hydrogenated derivatives (PHAH), and dinorcantharimide derivatives against a series of different microbial and mammalian cell types including fungi, bacteria, noncancerous mammalian cells, and cancerous mammalian cells. We then carried out time-dependent cell viability analysis against an opportunistic fungal pathogen (*Candida albicans*) of a Diels-Alder adduct (PHAH-EMAL), and N-ethyl maleimide (EMAL) was investigated in biological culture media to elucidate the effect of pH on the time-dependent toxicity of each compound. The effect of pH on the minimum inhibitory concentration (MIC) against *C.* albicans *and C. parapsilosis* showed the potential application of PHAH-EMAL as a pH-controllable pharmaceutical ingredient. Furthermore, we performed reaction kinetics analyses for the reaction system in the presence of a difunctional Diels-Alder adduct (PHAH-EMAL).

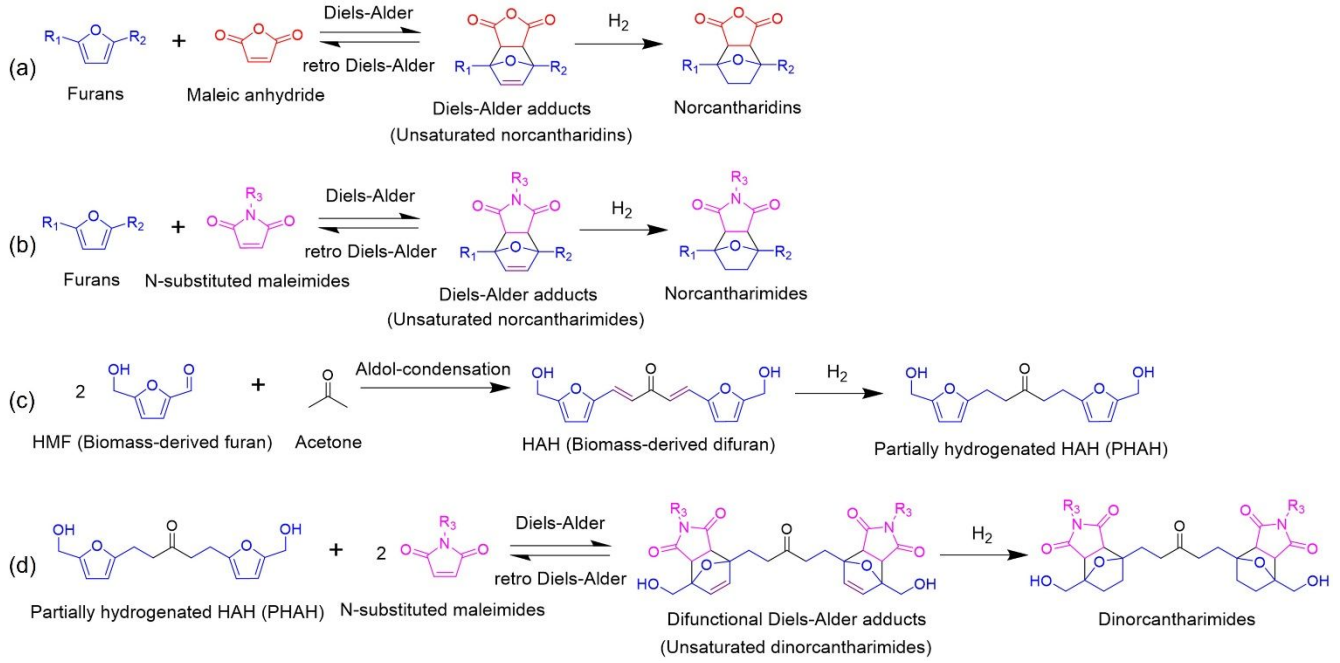

Scheme 1. Synthesis routes for (a) norcantharidins, (b) norcantharimides, (c) biomass-derived difuran, and (d) dinorcantharimides.

2. Experimental methods

2.1. Materials for biological samples and chemical synthesis of compounds. All mammalian cell lines were obtained from ATCC (Manassas, VA). 5-hydroxymethy furfural (HMF, AK Scientific, 98%), tetrahydrofuran (THF, Sigma-Aldrich, 250 ppm BHT as inhibitor, ACS reagent ≥99.0%), acetone (Fisher chemical, HPLC degree), NaOH (Honeywell, Reagent grade, pellets (anhydrous), ≥98%), HCl (Sigma-Aldrich, 37%), Mill-Q water (MQ water, ~18 MΩ cm), Cu/Al_2O_3 (Riogen, >98%, 5 wt% Cu loading). Ru/C (Sigma-Aldrich, 5wt% Ru loading), 2-propanol (IPA, Fisher chemical, HPLC degree), maleimide (MAL, Sigma-Aldrich, 99%), N-Ethylmaleimide (EMAL, Sigma-Aldrich, ≥99.0%), N-Benzylmaleimide (BMAL, Sigma-Aldrich, 99%), N-Hydroxymaleimide (HOMI, Sigma-Aldrich, 97%), 6-Maleimidohexanoic acid (Sigma-Aldrich, ≥98%), 3-Maleimidopropionic acid (N-Maleoyl-β-alanine, Sigma-Aldrich, 97%). The above chemicals and materials were used without further purification.

2.2. Synthesis of PHAH and FHAH from HMF (Entry 1-3 in Table 1)[25,26]. The aldol-condensed compound consisting of two HMF (5-hydroxymenthyl furfural) molecules and acetone is denoted as HAH. 1.83 g of NaOH was dissolved in 15 g of Milli-Q water to prepare 3 M of NaOH solution to catalyze aldol-condensation, and 2 mL of 37% HCl and 10 g of Milli-Q water were mixed to prepare 2 M of HCl solution to neutralize the NaOH catalyst after aldol-condensation. 10.2 g of HMF, 3 mL of acetone, and 71.28 mL of Milli-Q water were mixed in a 500 mL round bottom flask with magnetic stirring bar and placed in an oil bath at 35℃ for 5 min. 6.67 mL of 3 M of NaOH solution was added to the HMF and acetone solution, and the flask was capped with a glass lid. After one h of aldol-condensation, 7.74 mL of 2 M of HCl solution was added to the flask to terminate aldol-

condensation by neutralization. A pH strip was used to measure the pH of the aldol-condensed solution. The aldol-condensed solution with the precipitated HAH was vacuum filtered by paper while rinsing with ~300 mL of Milli-Q water. The washed HAH was dried in a vacuum oven at 50℃, under 500-600 mbar for 2 days. The product was characterized by ^{1}H and ^{13}C NMR (Figure S3).

Partially hydrogenated HAH is denoted as PHAH. The Cu/γ-Al_2O_3 catalyst (5 wt% Cu loading, 0.250 g of catalyst) was reduced at 300℃ (temperature was ramped from 22 to 300℃ for 2 h) for 1 h under 34 bar (at 22℃) of H_2 gas in a Parr reactor. The HAH feed solution was prepared by dissolving 1.12 g of HAH in an IPA/water cosolvent (IPA/water (mol) = 1/1, mixing 19.39 g (24.7 mL) of IPA solvent and 5.75 g (5.8 mL) of MQ water). The HAH feed solution was added by HPLC pump into the 50 mL Parr reactor, containing the reduced Cu/γ-Al_2O_3 catalyst under pressurized H_2 gas (~30 bar) to avoid catalyst oxidation by air. The reactor was purged twice with 50 bar of Ar gas and three times with 30 bar of H_2 gas. The reactor was pressurized to 35 bar of H_2 gas (at 22℃) and was heated to 120℃ in 35 min (final pressure increased to 45 bar at 120℃). The reactor was kept at 120℃ for 12 h with 450 rpm of stirring and cooled to room temperature by natural convection. The product solution was separated from the solid catalyst by syringe filter, and the cosolvent was evaporated by rotary evaporation (40℃, 30-100 mbar). The product was characterized by ^{1}H and ^{13}C NMR (Figure S4).

Fully hydrogenated HAH is denoted as FHAH. Ru/C catalyst (5 wt% Ru loading, 0.060 g of catalyst) with a magnetic stirring bar. HAH (0.46 g) was added into 30 mL of IPA solvent to prepare a feed solution and the HAH feed solution was added into the 50 mL Parr reactor. The reactor was purged twice with 50 bar of Ar gas and three times with 30 bar of H_2 gas. The reactor was pressurized to 30 bar of H_2 gas (at 22℃) and was heated to 180℃ in 60 min (final pressure increased to 55 bar at 180℃). The reactor was kept at 180℃ for 60 min with 450 rpm of stirring and cooled to room temperature by natural convection. The product solution was separated from the solid catalyst by a syringe filter, and IPA solvent was evaporated by rotary evaporation (40℃, 30-100 mbar). The product was characterized by ^{1}H and ^{13}C NMR (Figure S5).

2.3. Diels-Alder reaction of PHAH and N-substituted maleimides (Entry 4-8 in Table 1). The concentrations of PHAH and N-substituted maleimide were ~450 mM and ≥900 mM in THF (maleimide moiety/furan moiety ≥ 1.0), respectively, and the solution was placed in a glass-vial rector with lid and a magnetic stir bar. The well-capped reactor was kept at room temperature (22℃) with vigorous stirring for 5 days. THF solvent was evaporated by rotary evaporation (40℃, 30-100 mbar). When excess amounts of N-substituted maleimides were remained after the reaction, the Diels-Alder adducts were purified by chromatography separation. The product was characterized by ^{1}H and ^{13}C NMR (Figure S6-S10).

2.4. Hydrogenation of Diels-Alder adducts (Entry 9-11 in Table 1). The Diels-Alder adduct solution (~50 mM) was prepared in THF solvent. Controlled amounts (Diels-Alder adduct/catalyst (wt) = 5.80) of Ru/C catalyst and the feed solution were added into the 50 mL Parr reactor. The reactor was purged twice with 50 bar of Ar gas and three times with 30 bar of H_2 gas. The reactor was pressurized to 40 bar of H_2 gas (at 22℃) and was heated to 30℃ in 20 min (final pressure increased to 41 bar at 30℃). The reactor was kept at 30℃ for 900 min with 450 rpm of stirring and cooled to room temperature by natural convection. The product solution was separated from the solid catalyst by syringe filter, and THF solvent was evaporated by rotary evaporation (40℃, 30-100 mbar). The product was characterized by ^{1}H and ^{13}C NMR (Figure S11-S13).

2.5. Reaction kinetics analysis in water at 40℃. An aqueous solution with pH equal to 1 was prepared by adding 6N of HCl solution in MQ water and calibrated by pH meter (pH 1.07 at 24.7℃). 0.8 g amounts of Diels-Alder adducts (Entry 4, 7) were added to 2.8 g of MQ water or pH 1 aqueous solution in glass vial reactor with a magnetic stir bar. The reactor was kept at 40℃ in an oil bath with 500 rpm of stirring. 0.2 g (200 μL) of sample was collected at each time for kinetic analysis and diluted 2 times by adding 0.2 g (200 μL) of MQ water for HPLC analysis. Coupled differential equations (Eq.2-5) were used to formulate a kinetic model. The rate constants for retro Diels-Alder reaction (k_{-1}, k_{-2}), Diels-Alder reaction (k_1), and degradation (k_d) were measured by fitting the experimental reaction kinetics data to the model by MATLAB with 95% confidential intervals. The results of the reaction kinetics analyses are shown in Figure 1.

2.6. Reaction kinetics analysis in biological broths at 37℃ and maleimide exchange at 22℃. 0.056 g of PHAH-EMAL and 7.55 g of biological broth (pH 7.4, 6.0, or 5.0) were mixed in a glass vial reactor, and the reactor was kept at 37℃ in an oil bath with 600 rpm for 10 min. The saturated feed solution was separated from the insoluble precipitates of PHAH-EMAL by centrifuging at 2000 rpm for 5 min. The saturated feed solution was heated at 37℃ in an oil bath with 600 rpm for reaction kinetics measurements. 0.2 g (200 μL) of sample was collected at each time for analysis and diluted 2 times by adding 0.2 g (200 μL) of MQ water for HPLC analysis. The rate constants for retro Diels-Alder reaction (k_{-1}, k_{-2}), Diels-Alder reaction (k_1), and degradation (k_d) were measured by fitting the experimental reaction kinetics data to the kinetic model (Eq. 1-4) by MATLAB with 95% confidential intervals. The results of the reaction kinetics analyses are shown in Figure 3.

After 3 days reaction at 37℃, 2-3 mg of maleimide was added into the solution to carry out maleimide exchange experiments. The maleimide added solution was placed at room temperature (22℃) with vigorous stirring for the reaction. 0.2 g (200μL) of sample was collected at each time and diluted 2 times by adding 0.2 g (200μL) of MQ water for HPLC analysis to monitor the concentration change of each compound by maleimide exchange (Figure 4).

2.7. Materials for toxicity assays. Menadione and dibasic sodium phosphate were obtained from Millipore Sigma (Milwaukee, WI). 3-(N-Morpholino) propanesulfonic acid (MOPS) was obtained from Fisher Scientific (Pittsburgh, PA). 2,3-bis(2-methoxy-4-nitro-5-sulfophenyl)-2H-tetrazolium-5-carboxanilide (XTT) was purchased from Invitrogen. Gibco brand RPMI 1640 powder (containing phenol red and L-glutamine and without sodium bicarbonate or HEPES), Dulbecco's modified Eagle's medium (DMEM), Dulbecco's phosphate-buffered saline (DPBS, without calcium or magnesium), penicillin–streptomycin (10,000 U/mL), trypsin−EDTA (0.25%, with phenol red) were obtained from Thermo Fisher Scientific (Waltham, MA). Fetal bovine serum (FBS) was obtained from Peak Serum (Wellington, CO). Water (18.2 133 MΩ) was purified using a Millipore filtration system. Endothelial Cell Growth Medium-2 (EGM-2) and Mammary Epithelial Cell Medium (MEGM) were purchased from Lonza Bioscience (Walkersville, MD). Cell Titer Glo 2.0 assay kits were obtained from Promega (Madison, WI). Mueller Hinton Broth was

purchased from Fluka Chemicals (Switzerland). Citric acid was acquired from Acros Organics (Belgium).

2.8. Antifungal minimum inhibitory concentration (MIC) measurement. The antifungal activities of the compounds against *C. albicans* SC5314 cells at pH 7.4 were assayed in 96-well plates according to the planktonic broth microdilution susceptibility testing assay guidelines provided by the Clinical and Laboratory Standards Institute. The assay was modified to include a quantitative XTT assessment of cell viability. Two-fold serial dilutions (100 µL) of compounds in RPMI (pH adjusted to 7.4 with MOPS) were mixed with 100 µL of a *C. albicans* strain SC5314 cell suspension (grown for 24 h at 30 °C and concentration adjusted to 5 × 10^3 cells/mL), and the plates were incubated at 37 °C for 48 h. Wells lacking compound (cell controls) and wells lacking both compounds and cells (medium sterility controls) were included in every plate that was assayed. After 48 h, 100 µL of XTT solution (0.5 g L–1 in PBS, pH 7.4, containing 3 µM menadione in acetone) was added to all wells, and plates were incubated at 37 °C in the dark for 1.5 hours, and absorbance measurements at 490 nm were recorded using a plate reader. The cell viability was plotted as a function of compound concentration. Percent cell viability was calculated by Equation 1 where A_{490}, $A_{490}^{\text{cell control}}$, and $A_{490}^{\text{background}}$ are the average absorbance values at 490 nm of the supernatant from wells containing a specific concentration of compound, wells with positive cell control, and medium sterility control wells, respectively. Experiments were performed in technical duplicates. The lowest assayed concentration of compound that resulted in a decrease in normalized absorbance of at least 90% of the mean was taken as the minimum inhibitory concentration (MIC) of that compound. DMSO vehicle controls were added for comparison. (Figure S14).

$$\text{cell viability } (\%) = \frac{\left(A_{490} - A_{490}^{\text{background}}\right)}{A_{490}^{\text{cell control}} - A_{490}^{\text{background}}} \times 100 \quad \text{.....Eq.1}$$

For pH-dependent antifungal MIC determination against multiple fungal species, the general procedure for MIC determination as described above was followed with modifications. For each pH condition, two-fold serial dilutions (100 µL) of PHAH-EMAL and EMAL were prepared in RPMI media (pH adjusted to 5, 6, and 7.4 with citric acid and dibasic sodium phosphate, according to McIlvaine buffer guidelines). *C. albicans* (SC5314), *C. parapsilosis* (5986), and *C. tropicalis* (98-234) cell suspensions adjusted to 5 × 10^3 cells/mL at each assayed pH were added (100 µL) to the wells with the corresponding pH and assayed under 37 °C for 48 hours. (Figure S20-S23)

2.9. Antibacterial MIC assay of compounds. The antibacterial activities of the compounds against *S. aureus* ATCC 3359 were assayed in 96-well plates according to the planktonic broth microdilution susceptibility testing assay guidelines provided by the Clinical and Laboratory Standards Institute. The assay was modified to include a quantitative XTT assessment of cell viability. Two-fold serial dilutions (100 µL) of compounds in Mueller-Hinton Broth medium were mixed with 100 µL of an *S. aureus* cell suspension (grown for 24 h at 37 °C and concentration adjusted to 1 × 10^6 cells/mL based on solution optical density at 600nm), and the plates were incubated at 37 °C for 24 h. Wells lacking compound (cell controls) and wells lacking both compounds and cells (medium sterility controls) were included in every plate that was assayed. After 24 hours, 100 µL of XTT solution was added in the same manner as for antifungal MIC assays described above, and the MIC was determined based on 90% reduction of normalized absorbance, consistent with the antifungal assays. DMSO vehicle controls were added for comparison. (Figure S15).

2.10. Mammalian cell toxicity assays. All cell culture maintenance and cytotoxicity assays were performed in 37°C and 5% CO_2. 3T3 mouse fibroblast (NIH/3T3) cells and MDA-MB-231 triple-negative human breast cancer cells were cultured in DMEM containing 10% (v/v) fetal bovine serum, 100 µg/mL streptomycin, and 100 units/mL penicillin. Human umbilical vein-endothelial cells (HUVECs) were grown in EGM-2 Bullet Kit media. MCF-10A non-tumorigenic mammary epithelial cells were cultured in MEGM Bullet Kit media. Cells were passaged upon 70−80% confluency by gently washing the cell layer with PBS and then detaching them from the bottom of the wells with a 0.25% trypsin−EDTA solution. For mammalian cytotoxicity experiments, confluent cells from an ongoing cell line were detached during passaging and seeded onto 96 well plates at a density of 25,000 cells/mL in 100 µL of medium in each well and then maintained for 24 h. Following incubation, serial dilutions of compounds in 100 µL of media were added to each well and were incubated for another 48 hours. Mammalian cell viability was characterized using a Cell Titer Glo metabolic activity assay. Cell Titer Glo assay was performed according to the manufacturer's recommendations by adding 100 µL of reagent to each of the wells. Next, 100 µL of supernatant in each well was transferred into an opaque-bottomed white 96-well plate and the luminescence signal was quantified. Background luminescence from wells containing medium and Cell Titer Glo was subtracted from all readings and data were normalized relative to the DMSO vehicle control. Experiments were performed in technical duplicates or more. The assayed concentration of compound that resulted in a decrease in normalized luminescence of at least 90% of the mean was taken as the IC_{90} (Concentration at which 90% or more cell viability is reduced compared to the control) of that compound. (Figure S16-S19).

2.11. Time-Kill curves of C. albicans against compounds. We measured the colony forming units of *C. albicans* over time when exposed to PHAH-EMAL and EMAL to evaluate the time-dependent behavior of compounds of interest and to identify the effects of pH. 2 mL of *C. albicans* inoculum (5 × 10^3 cells/mL) in RPMI (pH adjusted to 5, 6, and 7.4 with citric acid and dibasic sodium phosphate) at different pH values were added to each well of a 6-well plate, and an additional 2mL of compounds in the same corresponding pH in RPMI media were added. Concentrations of each compound incubated were 256 µg/mL and 16 µg/mL each for PHAH-EMAL and EMAL respectively. A DMSO vehicle control was included for all pH values and tested as comparison. At each time point, a small volume (50 µL) was removed in duplicate and serially diluted before plating on YPD agar plates for colony counting. The YPD plates were incubated for 48 hours and the number of colony forming units (CFU) on the plates were counted. At each time point, the average number of colony-forming units was determined from the two technical duplicates.

3. Results and discussion

3.1. Effect of molecular structure on toxicity against microorganisms

Aldol condensation of biomass-derived 5-hydroxymethyl furfural (HMF) and acetone yielded a symmetric molecule with a difuran functionality, denoted as HAH (HMF-Acetone-HMF). The selective hydrogenation of C=C bond in HAH produced an electron-rich difuran compound (PHAH). PHAH has furan moieties that are isolated from the electron-withdrawing carbonyl group. This furan moiety thereby becomes electron-rich for Diels-Alder reaction with electron-deficient maleimide, allowing the formation of a norcantharimide functionality. A variety of norcantharimide derivatives were then synthesized by Diels-Alder reaction of PHAH with N-substituted maleimides as shown in Table 1. The molecular structures of the compounds in Table 1 were characterized by ^{13}C qNMR and 2D HSQC NMR in Figure S3-S13. We examined the toxicity of these adducts against different types of cells, including fungi (*Candida albicans*), bacteria (*Staphylococcus aureus*), cancerous cells (*MDA-MB-231* triple-negative breast cancer cell line), and noncancerous mammalian cells (*NIH-3T3* mouse fibroblasts, *MCF-10A* mammary epithelial cells, human umbilical vein endothelial cells (*HUVECs*). The toxicity assays were performed by measuring the inhibition concentration (MIC for bacteria and fungi, IC_{90} for mammalian cells) of each compound against different cell types, where lower values represent higher toxicities of the compounds. Table 1 shows the structural effects on the toxicity of the biomass-derived small molecules (Entry 1-11) against different cell types. The existence of C=C bonds causes an increase in toxicity against the cells investigated. The toxicities of the monomers decreased as the degree of hydrogenation of HAH increases (Entries 1-3). Entries 10 and 11 are the hydrogenated products of the compounds in Entry 7 and 8 respectively. The toxicity difference between Entry 7 and 10 (or Entry 8 and 11) showed that the toxicity against all cell types decreased when the C=C bonds are hydrogenated. The higher toxicities of the unsaturated compounds than those of the hydrogenated compounds are consistent with previous literature, where the presence of antibonding molecular orbitals (LUMO) in C=C bonds provide an active site for nucleophilic attack, which could potentially influence toxicity against cells.[12] Additionally, increasing the hydrophobicity of N-substitution in Entries 6-8 decreases both MIC and IC_{90}. When amino acids such as alanine (Entry 4) and 6-aminocaprotic acid (Entry 5) were appended onto the maleimide, the longer alkane length from $-C_2H_4$ (Entry 4) to $-C_5H_{10}$ (Entry 5) in amino acids decreased both MIC and IC_{90} values. These results indicate that the increasing hydrophobicity of N-substitutions in the maleimide moiety contributes to a higher toxicity. The effect of higher toxicities from hydrophobic N-groups were observed by the hydrogenated Diels-Alder adducts in Entry 9-11. Consequently, the toxicity of biomass-derived small molecules can be engineered through hydrogenation and Diels-Alder reactions with N-substituted maleimides.

Table 1. Toxicities of biomass-derived compounds against different cell types; S. aureus (bacterium), C. albicans (fungus), NIH-3T3 (mouse fibroblast), HUVEC (human endothelial cells), MDA-MB-231 (human breast cancer cells), and MCF-10A (non-cancerous mammary epithelial cells). (MIC: minimum inhibition concentration, IC_{90}: 90% cell viability inhibition concentration; N.A. represents no activity)

Entry	Compounds	Structure	Cell type					
			MIC (μg/mL)		IC_{90} (μg/mL)			
			S. aureus (ATCC 3359)	*C. albicans (SC5314)*	*NIH-3T3*	*HUVEC*	*MDA-MB-231*	*MCF-10A*
		Biomass-derived difuran compounds						
1	HAH	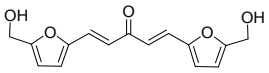	N.A.	N.A.	16	16	128	32
2	PHAH	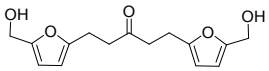	N.A.	N.A.	128	256	512	128
3	FHAH	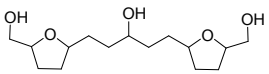	N.A.	N.A.	>1024	>1024	N.A.	1024
		Diels-Alder adducts (Unsaturated dinorcantharimides)						
4	PHAH-Amino Acid 1	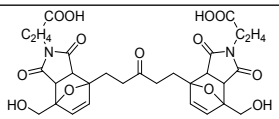	N.A.	N.A.	512	1024	N.A.	512
5	PHAH-Amino Acid 2	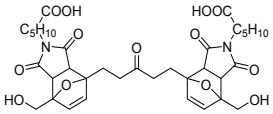	N.A.	N.A.	N.A.	256	>1024	128
6	PHAH-HOMI	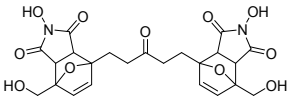	N.A.	>1024	>1024	>1024	N.A.	>1024
7	PHAH-EMAL	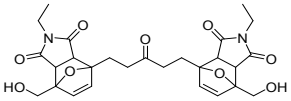	>1024	512	64	128	256	32
8	PHAH-BMAL	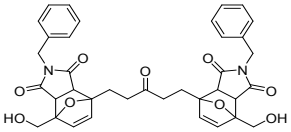	1024	256	32	32	128	64
		Hydrogenated Diels-Alder adducts (dinorcantharimides)						
9	PHAH-MAL-H	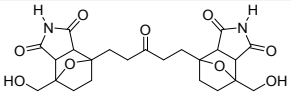	N.A.	N.A.	>1024	N.A.	N.A.	1024
10	PHAH-EMAL-H	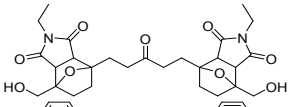	N.A.	>1024	>1024	>1024	>1024	512
11	PHAH-BMAL-H	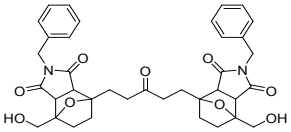	N.A.	N.A.	1024	256	512	256

3.2. Effect of pH on toxicity of difunctional Diels-Alder adducts

3.2.1. Reaction kinetics analyses for retro Diels-Alder reaction

In Table 1, the toxicity difference between difurans (Entry 1,2) and difunctional Diels-Alder adducts (Entry 4-8) implies that the retro Diels-Alder reaction of Diels-Alder adducts can be used to control the chemical toxicity by releasing PHAH and maleimides. The different pH values of the solution were used to demonstrate the catalytic effect of pH on the retro Diels-Alder reaction. The pathway for the retro Diels-Alder of the Diels-Alder adducts, such as PHAH-EMAL (Entry 7) and PHAH-Amino acid 1 (Entry 4) at 40℃ is displayed in Figure 1a. Equation 2 represents the concentration profile of the Diels-Alder adduct (PHAH-EMAL) by retro Diels-Alder reaction (k_{-1}), Diels-Alder reaction (k_1) and degradation (k_d). Equations 3 and 4 describe the formation and deformation of maleimide (EMAL) and intermediate by retro Diels-Alder reaction (k_{-1}, k_{-2}) and Diels-Alder reaction (k_1). Equation 4 shows the degradation (k_d) of the Diels-Alder adduct (PHAH-EMAL). Comparison of Figure 1b and d shows the increasing yield (from 9 to 45 mol%) of N-ethyl maleimide (EMAL) from PHAH-EMAL by decreasing the pH from 7 to 1 at 40℃ in water. The degree of retro Diels-Alder reaction can be assessed by the ratio

between the summation of rate constants for retro Diels-Alder reaction (k_{-1}+k_{-2}) to the rate constant for Diels-Alder reaction (k_1), denoted as the value of (k_{-1}+k_{-2})/k_1 (unit: mM). The value of (k_{-1}+k_{-2})/k_1 for PHAH-EMAL (Entry 7) was 5.78 mM under pH 7 at 40℃ (Figure 1b), whereas (k_{-1}+k_{-2})/k_1 was calculated to be 32.4 mM under pH 1 at 40℃ (Figure 1c). The Brønsted acid not only catalyzed the retro Diels-Alder reaction[18,27] but also enabled the degradation of PHAH-EMAL (k_d=0.0061±0.0010 h^{-1}) as a side reaction, which resulted in lack of equilibrium between Diels-Alder and retro Diels-Alder reactions. We note that the intermolecular Brønsted acid from propionic acid moiety in PHAH-Amino Acid 1 (Entry 4) increased the summation of rate constants for retro Diels-Alder reaction (k_{-1}+k_{-2}) from 0.0052 h^{-1} (Figure 1b) to 0.0115 h^{-1} (Figure lc), but the intermolecular Brønsted acid did not increase the degree of retro Diels-Alder reaction for PHAH-Amino Acid 1 ((k_{-1}+k_{-2})/k_1 =3.83 mM), compared to PHAH-EMAL under pH 7 ((k_{-1}+k_{-2})/k_1 =5.78 mM). This result implies that the intermolecular Brønsted acid cannot disturb the equilibrium between Diels-Alder and retro Diels-Alder reaction because it does not cause side reactions. The external Brønsted acid (pH 1) can drive both retro Diels-Alder reaction and degradation of PHAH-EMAL which can give rise to higher yield of EMAL by perturbing the thermodynamic equilibrium of the reaction system. Accordingly, the degree of retro Diels-Alder reaction can be controlled by changing the pH of the solution. The rate constant with the wide confidence interval greater than the mean value indicates that the regressed rate constant is statistically less significant by using 4-7 data points to fit the presented 4-step reaction mechanism. Since the rates of retro Diels-Alder reaction were slow and the release of maleimides occurred over a few days, these values are interpreted to have low or near zero rate constants for the time ranges examined. Thus, the calculation error associated with the value consistently became larger, as the model struggled to calculate near zero values.

$$\frac{d[PHAH\text{ - }EMAL]}{dt} = -k_{-1}[PHAH\text{ - }EMAL] + k_1[intermediate][EMAL] - k_d[PHAH\text{ - }EMAL] \quad \text{Eq.2}$$

$$\frac{d[EMAL]}{dt} = k_{-1}[PHAH\text{ - }EMAL] - k_1[intermediate][EMAL] + k_{-2}[intermediate] \quad \text{Eq.3}$$

$$\frac{d[Int.]}{dt} = k_{-1}[PHAH\text{ - }EMAL] - k_1[intermediate][EMAL] - k_{-2}[intermediate] \quad \text{Eq.4}$$

$$\frac{d[Degraded\ PHAH\text{ - }EMAL]}{dt} = k_d[PHAH\text{ - }EMAL] \quad \text{Eq.5}$$

(The units of k_{-1}, k_{-2}, k_d are h^{-1}, the unit of $k_1$is $mM^{-1}\cdot h^{-1}$)

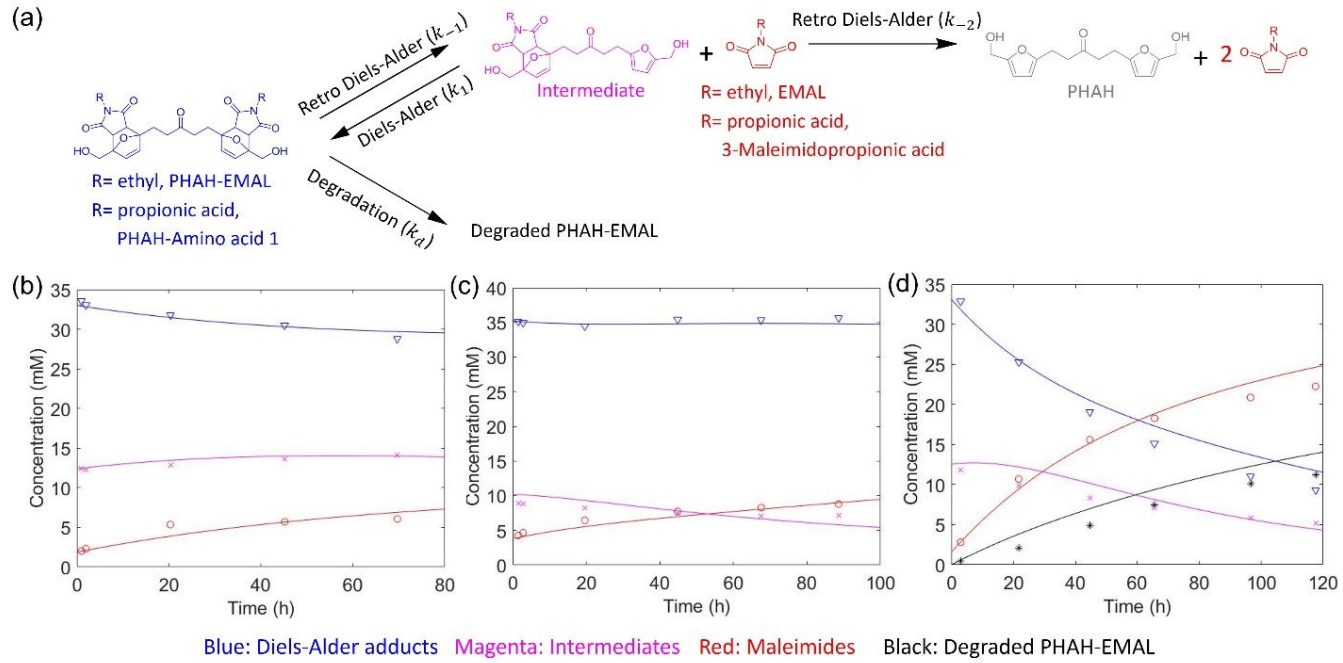

Figure 1. (a) Reaction pathways for the decomposition of Diels-Alder adducts by retro Diels-Alder reaction and degradation; Reaction kinetics analysis of Diels-Alder adducts with different N-substitutions and under different pH conditions, (b) -R group is ethane (Entry7, PHAH-EMAL) under pH7.0 (k_{-1}=0.0034 ± 0.0027 h^{-1}, k_1= 0.0009 ± 0.0013 $mM^{-1}h^{-1}$, k_{-2}= 0.0018 ± 0.0009 h^{-1}), (c) -R group is propionic acid (Entry 4, PHAH-Amino acid 1) under pH 7.0, (k_{-1}= 0.0047 ± 0.0197 h^{-1}, k_1= 0.0030 ± 0.0131 $mM^{-1}h^{-1}$, k_{-2}= 0.0068 ± 0.0017 h^{-1}) and (d) -R group is ethane (Entry 7, PHAH-EMAL) under pH 1.0 (k_{-1}= 0.0076 ± 0.0053 h^{-1}, k_1= 0.0007 ± 0.0008 $mM^{-1}h^{-1}$, k_{-2}= 0.0150 ± 0.0035 h^{-1}, k_d=0.0061 ± 0.0010 h^{-1}) at 40°C in water solvent (The calculated rate constants was bounded within 95% confidential interval).

3.2.2 pH effect on pharmacokinetics of maleimide and Diels-Alder adduct

The results shown in Figure 1 indicate that the pH of the solution affects the degree of retro Diels-Alder reaction and the release of maleimides. A time-kill assay was then performed to characterize the potential time-scale dependent toxicity of compounds against a model pathogen at different pH values which affect the degree of retro Diels-Alder reaction to release chemicals (i.e., maleimide, intermediate, PHAH). A Diels-Alder adduct (PHAH-EMAL) and a maleimide (EMAL) were investigated to quantify the pH effect on the

toxicity against *C. albicans,* an opportunistic fungal pathogen, in Figure 2. The time-kill assay showed that 16 μg/mL of EMAL eradicated *C. albicans* within 3 hours at all conditions with the fastest eradication times at pH 7.4 (Figure 2a). Meanwhile, PHAH-EMAL required more than 4 hours to kill cells, even though its concentration was 16-fold higher (256 μg/mL) than that of EMAL (16 μg/mL), with pH 6 conditions eradicating the cells the fastest (Figure 2b). We hypothesize that the faster cell killing of EMAL at pH 7.4 influences the toxicity kinetics of PHAH-EMAL at different pH conditions. For example, from our previous chemical reaction kinetics analysis (Figure 1), we hypothesize EMAL to be released from PHAH-EMAL at higher concentrations in lower pH conditions. However, since EMAL eradicates cells faster in a higher pH (Figure 2a), there could be a trade-off between the release of EMAL and inherent cell killing speed of EMAL. This trade-off may lead to the fastest cell killing for PHAH-EMAL at the pH 6.0 condition. Accordingly, the pH dependent toxicity of the Diels-Alder adduct could be a result of a Br*ϕ*nsted acid-catalyzed retro Diels-Alder reaction (Figure 1) that increases the release of a more toxic chemical appended to it (EMAL, for example) as pH decreases.

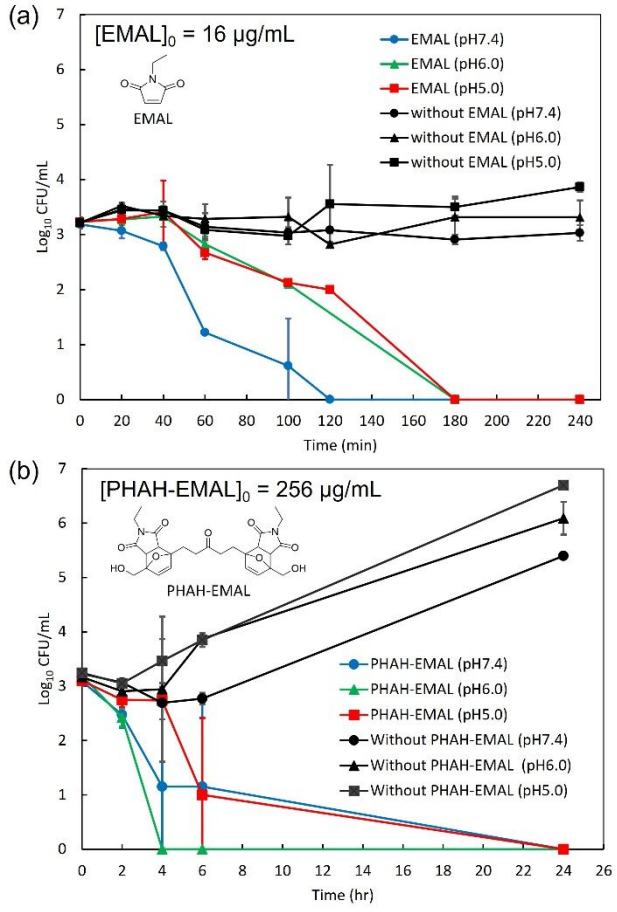

Figure 2. Pharmacokinetics analysis of (a) EMAL (16 μg/mL) and (b) PHAH-EMAL (256 μg/mL) against a fungus (*C. albicans*) under different pH conditions. CFU is the colony forming units of *C. albicans* counted on agar. Data points are the average of two technical replicates each, and error bars indicate standard deviations.

3.2.3. pH effect on rate constants for the release of maleimide

Reaction kinetics analyses were carried out to address the potential factors that drive the pH-dependent pharmacokinetics of PHAH-EMAL in Figure 2. For the analyses, cell-free reaction kinetics were analyzed under the biological conditions that were used for the pharmacokinetics experiments in Figure 3. The mean values of the regressed rate constants at different pH values are summarized in Table S1. The value of $(k_{-1}+k_{-2})/k_d$ was used to compare the degree of retro Diels-Alder reaction ($k_{-1}+k_{-2}$) against the chemical degradation (k_d). $(k_{-1}+k_{-2})/k_d$ was 0.89, 5.92, and 19.8 under pH 7.4, 6.0, and 5.0 buffer, respectively. The lowest value of $(k_{-1}+k_{-2})/k_d$ in pH 7.4 buffer illustrated that the degradation of PHAH-EMAL was significant in pH 7.4 buffer because the higher concentration of Na_2HPO_4 in pH 7.4 buffer compared to the lower pH buffers (Table S2) may degrade PHAH-EMAL by oxidation.[28–30] The value of $(k_{-1}+k_{-2})/k_1$ represents the equilibrium constant of Diels-Alder (k_1) and retro Diels-Alder reaction ($k_{-1}+k_{-2}$) under the different pH buffer. The equilibrium constant was 0.41, 0.24, and 0.37 mM at pH 7.4, 6.0, and 5.0 buffer respectively, and it shows that $(k_{-1}+k_{-2})/k_1$ was not significantly affected by pH in biological broths. However, the released amounts of EMAL from PHAH-EMAL increased by 0.0, 4.0, and 8.4 mol% as pH decreased by 7.4, 6.0, and 5.0, respectively. These results show that the combination of the increased retro Diels-Alder reaction and the suppressed degradation can result in the higher yield of EMAL at lower pH conditions. Therefore, the pH-dependent balance between Diels-Alder equilibrium and the chemical degradation is of critical importance to understand the release of maleimides from the Diels-Alder adducts in both biological broths (Figure 3) and water (Figure 1).

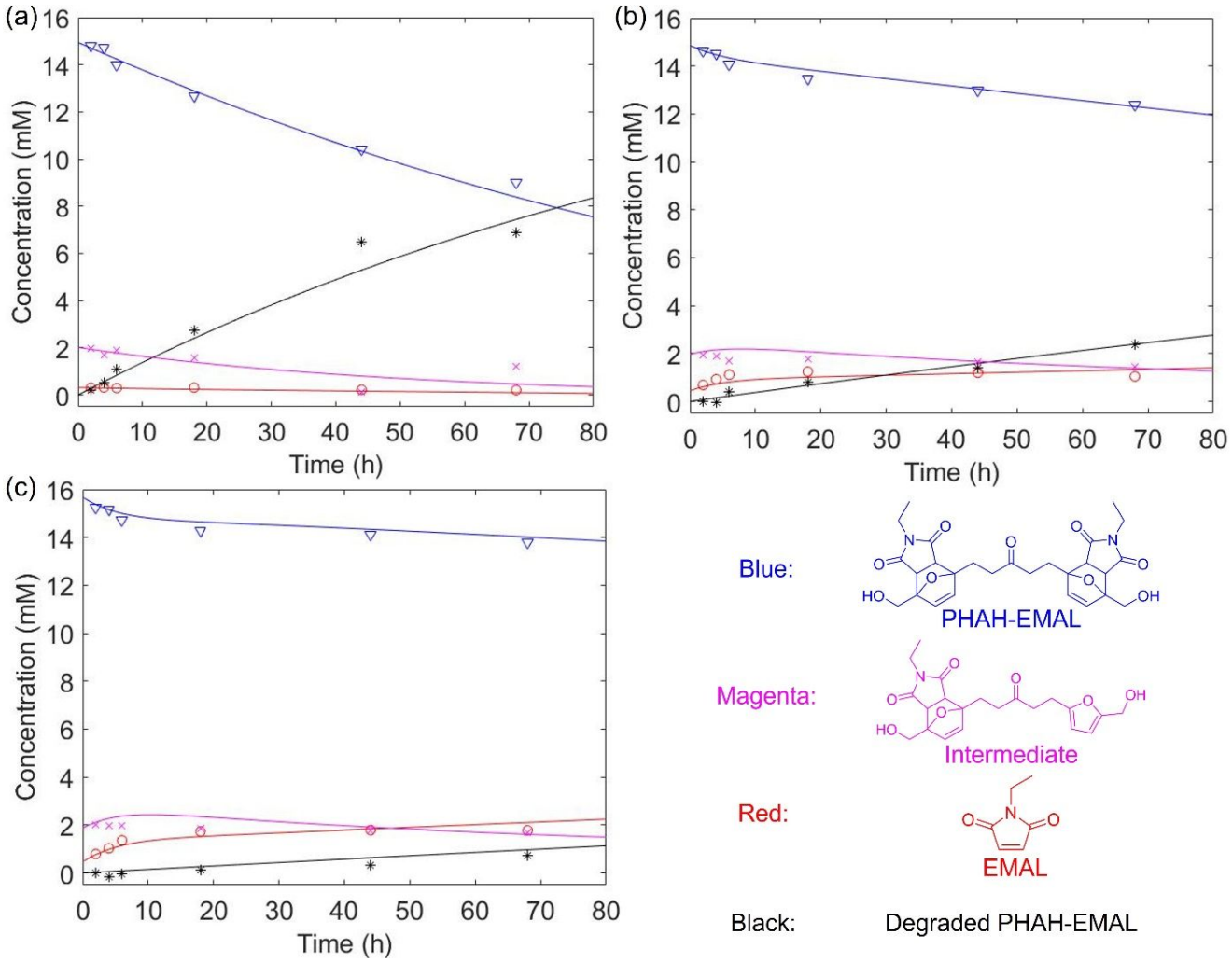

Figure 3. Reaction kinetics analysis for Diels-Alder, retro Diels-Alder reaction and degradation of PHAH-EMAL under (a) pH 7.4 (k_{-1}= 0.0007 ± 0.0033 h^{-1}, k_1= 0.0206 ± 0.1498 $mM^{-1}h^{-1}$, k_{-2}= 0.0092 ± 0.0085 h^{-1}, k_d= 0.0096 ± 0.0009 h^{-1}), (b) pH 6.0 (k_{-1}= 0.0095 ± 0.0113 h^{-1}, k_1= 0.0646 ± 0.0828 $mM^{-1}h^{-1}$, k_{-2}= 0.0059 ± 0.0026 h^{-1}, k_d= 0.0026 ± 0.0003 h^{-1}), and (c) pH 5.0 (k_{-1}= 0.0130 ± 0.0083 h^{-1}, k_1= 0.0535 ± 0.0398 $mM^{-1}h^{-1}$, k_{-2}= 0.0068 ± 0.0026 h^{-1}, k_d= 0.0010 ± 0.0003 h^{-1}) at 37℃ in biological broths (The calculated rate constants were bounded within 95% confidential interval).

We note that the initial concentration of PHAH-EMAL (~15 mM) for the reaction kinetics analyses was 16 times higher than the concentration that was used for the time-kill assays (256 μg/mL=0.92 mM) in Figure 2 due to the sensitivity limit of the analytical instrument (HPLC). Thus, the reaction kinetics model was used to predict the yield of EMAL from PHAH-EMAL at the concentration of the time-kill experiments (Figure S2). As the feed concentration decreased from 15 mM to 0.92 mM, the yield of EMAL increased from 0.0, 4.0, 8.4 mol% to 4.7, 36.3, 48.3 mol% under pH values of 7.4, 6.0, 5.0, respectively. Accordingly, the PHAH moiety in the Diels-Alder adducts could deliver more maleimides at the dilute concentration, and PHAH can potentially be useful for prodrug applications by controlling the release of therapeutic maleimides[11,12] at sites with lower pH, such as large volume tumors.[20]

3.3. Applications of Diels-Alder adduct as potential pharmaceutical ingredient

3.3.1 pH-controlled antifungal activity of Diels-Alder adduct

The antifungal activity of the Diels-Alder adduct was measured at different pH values to demonstrate a prodrug application in the pharmaceutical field. The dependence of the toxicity of PHAH-EMAL with respect to pH for different opportunistically pathogenic fungi was additionally investigated and is summarized in Table 2. The MIC for PHAH-EMAL showed a pH-dependence against both *C. albicans* and *C. parapsilosis*, while the MIC of EMAL was 4 μg/mL regardless of pH and the type of fungi. The independence of the toxicity of EMAL with respect to pH is consistent with the results from the time-kill assay in Figure 2b and can be explained by the high toxicity of EMAL that kills cells before significant cell growth. The lower MIC of PHAH-EMAL against *C. albicans* and *C. parapsilosis* at the lower pH conditions (pH 6.0 and 5.0) may result from acid-catalyzed retro Diels-Alder reactions that releases the cytotoxic EMAL to the surroundings. However, *C. tropicalis* did not show pH-dependent MIC changes, which implies that there could be additional biological factors that affect the MIC other than the chemical toxicity. Since these results show a potential pH-reactive difference in compound toxicity for certain fungal pathogens (against *C. albicans* and *C. parapsilosis*)[31], further efforts should focus on elucidating the

mechanism of action behind the species-dependent effect of pH on PHAH-EMAL activity.

Table 2. Toxicity of PHAH-EMAL and EMAL against fungi (*C. albicans*, *C. parapsliosis*, *C. tropicalis*) measured by MIC under different pH conditions. The errors are the standard deviations of MIC values from a minimum of two independent experiments.

pH	Antifungal MIC (μg/mL)		
	C. albicans (SC5314)	*C. parapsilosis* (5986)	*C. tropicalis* (98-234)
	PHAH-EMAL		
7.4	427 ± 148	384 ±181	384 ± 181
6.0	107 ± 37.0	64 ± 0	384 ± 181
5.0	192 ± 111	64 ± 0	384 ± 181
	EMAL		
7.4	4	4	4
6.0	4	4	4
5.0	4	4	4

3.3.2. Delivery of maleimide by dynamic equilibrium of Diels-Alder reaction

Difunctional Diels-Alder adducts could be used in drug delivery applications since the release of toxic cargo molecules can be controlled by targeted pH conditions. We hypothesize that the retro Diels-Alder reaction of PHAH-EMAL can release EMAL as a cargo molecule. The pH of the biological broths affected the following reactions (Figure 4a): (i) Diels-Alder reaction of the released PHAH, (ii) dynamic equilibrium of maleimide exchange, and (iii) degradation of compounds. At pH 7.4 (Figure 4b), there was a gradual degradation of exo-PHAH-EMAL during the retro Diels-Alder reaction at 37℃ for 0-68 h. 8 mM of maleimide (MAL) was added after the retro Diels-Alder reaction to induce the maleimide exchange in the Diels-Alder adduct. As a result, the concentration of exo-PHAH-EMAL decreased from 6 to 4 mM and the 2 mM of PHAH-MAL was produced. The conserved amounts of the decreased exo-PHAH-EMAL and the increased PHAH-MAL implies that PHAH-EMAL was converted to PHAH-MAL by dynamic equilibrium of maleimide exchange between EMAL and MAL. Also, there was a significant decrease of the MAL concentration by degradation. Thus, maleimide degradation and the dynamic equilibrium of Diels-Alder reaction were dominant reactions in pH 7.4 broth. When the pH of biological broth was 6.0 (Figure 4c), 1.5 mM of EMAL was formed by retro Diels-Alder reaction of PHAH-EMAL for 0-68 h at 37℃. After adding 10 mM of MAL, 2 mM of PHAH-MAL was formed, and the concentration of MAL decreased from 10 to 4 mM. The formation of PHAH-MAL (2 mM) is higher than the released amounts of EMAL (1.5 mM) by retro Diels-Alder reaction. This behavior implies that there was not only Diels-Alder reaction of MAL and PHAH, but also dynamic equilibrium by maleimide exchange to convert PHAH-EMAL to PHAH-MAL. Furthermore, degradation of MAL was observed during the Diels-Alder reaction in pH 6.0 broth. The degradation reactions of PHAH-EMAL and MAL were not significant under pH 5.0 condition (Figure 4d). Accordingly, 2.4 mM of EMAL was released during the retro Diels-Alder reaction at 37℃ and 4 mM of MAL was consumed by Diels-Alder reaction and degradation to produce 2 mM of PHAH-MAL when 18 mM of MAL was added to the system. We note that endo-PHAH-EMAL was not quantified by HPLC analysis because of the peak overlap between the endo-conformation and maleimide (Figure S1). Therefore, these results are consistent with the view that the change in effective toxicity of the Diels-Alder adduct resulted from the retro Diels-Alder reaction, releasing the maleimide compound.

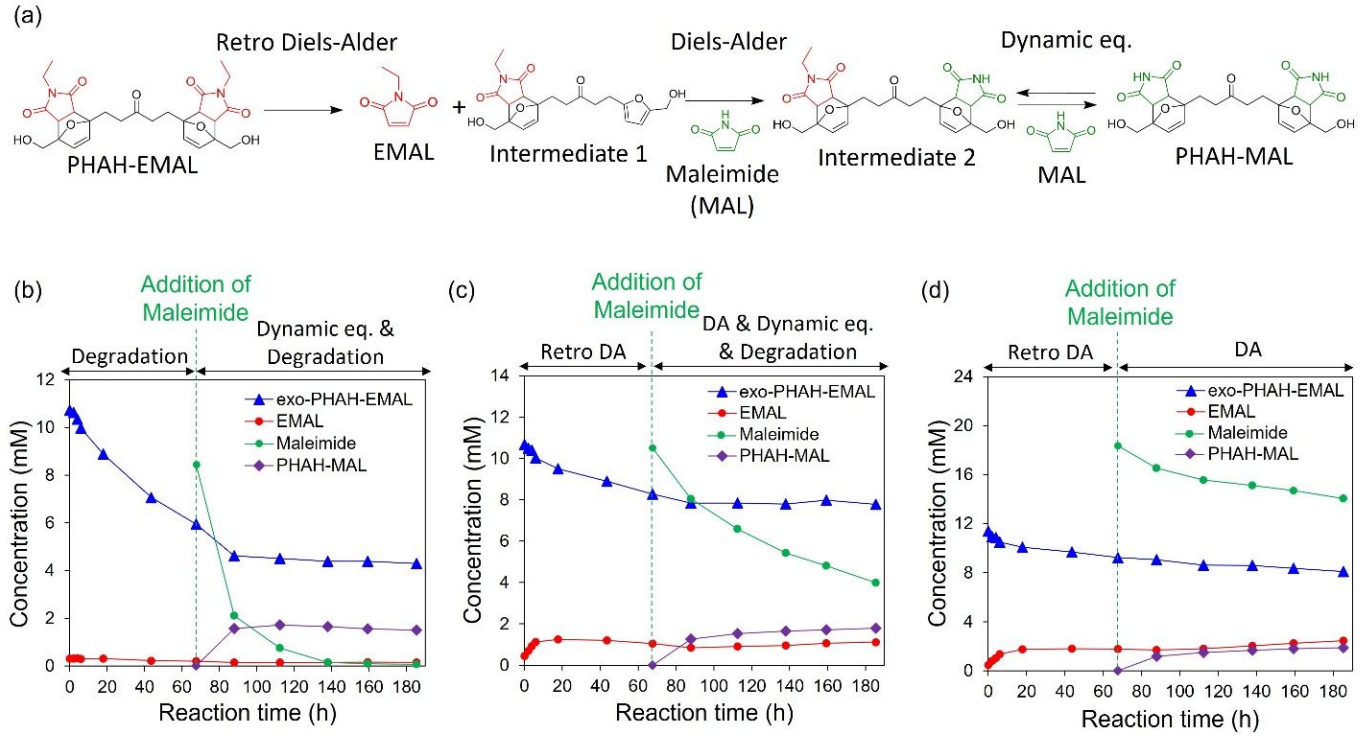

Figure 4. (a) Scheme for reaction pathways for maleimide exchange; concentration profile of exo-PHAH-EMAL, EMAL, maleimide, and PHAH-MAL under (b) pH 7.4, (c) pH 6.0, and (d) pH 5.0 in biological broth (For 0-68 h, retro Diels-Alder reaction occurred at 37℃ and maleimide exchange occurred at 22℃ from 68 to 185 h).

ARTICLE

4. Conclusions

A biomass-derived difuran molecule, denoted as PHAH, can undergo Diels-Alder reactions with N-substituted maleimides to produce biologically active norcantharmides. C=C bonds can serve as potential nucleophilic attack sites in molecular structures of the corresponding biomass-derived small molecules and contribute to higher toxicity against different cell types. Additionally, increased hydrophobicity from N-substitution of the maleimide moiety in the Diels-Alder adducts contributes to the higher toxicity of the compounds against different cell types. The difuran PHAH compound can serve as a cargo platform for delivering maleimide-based pharmaceutical compounds by Diels-Alder reaction, and an acid-catalyzed retro Diels-Alder reaction can be used to control the release of maleimide-based drugs at ambient body temperature. Furthermore, we demonstrated that amino acids such as alanine (Entry 4) and 6-aminocaprotic acid (Entry 5), can be substituted into the N-atom site in the maleimide. The carboxylic acid moiety of these amino acid-substituted maleimides provides a site to potentially append antibodies to form antibody-drug conjugates, which have been known for their use in anticancer applications, opening possibilities for further modifications to enhance targeted selectivity.[11] This biomass-based synthesis platform can supply therapeutic small molecules in a sustainable manner, and the control of Diels-Alder, retro Diels-Alder, and hydrogenation reactions can be used to manipulate the activity of the compounds for various biomedical applications, such as pH-responsive prodrugs.

5. Author Contributions

Conceptualization: HC, GWH, JAD; Methodology: HC, DHC, AGS; Investigation: HC, DHC, AGS; Visualization: HC, DHC, DML, SPP, GWH, JAD; Funding acquisition: DML, SPP, GWH, JAD; Project administration: JAD; Supervision: GWH, DML, SPP, JAD; Writing: HC, DHC, AGS, GWH, DML, SPP, JAD.

6. Conflicts of interest

There are no conflicts to declare.

7. Acknowledgement

This material is based upon work supported in part by the U.S. Department of Energy, Office of Science, Office of Basic Energy Sciences, Chemical Sciences, Geosciences, and Biosciences Division, under Contract DE-SC0014058; Great Lakes Bioenergy Research Center, U.S. Department of Energy, Office of Science, Office of Biological and Environmental Research under Award Number DE-SC0018409; and National Institutes of Health under Award Numbers 5T32GM135066-02 and R33AI127442. Alexios G. Stamoulis was funded by the National Science Foundation, through grant CHE-1953926. We thank Prof. Shannon Stahl (Department of Chemistry, UW-Madison) for use of chemical purification resources in his lab. The NMR facilities: Bruker Quazar APEX2 and Bruker Avance-500 were funded by a generous gift from Paul J. and Margaret M. Bender; Bruker Avance-600 was funded by NIH S10 OK012245; Bruker Avance-400 was funded by NSF CHE-414 1048642 and the University of Wisconsin-Madison. **Data and materials availability:** All data are available in the main text or the supporting information.

8. Note and references

1 H. Chang, G. W. Huber and J. A. Dumesic, *ChemSusChem*, 2020, **13**, 5213–5219.
2 M. Gregoritza and F. P.Brandl, *Eur. J. Pharm. Biopharm.*, 2015, **97**, 438–453.
3 V. Froidevaux, M. Borne, E. Laborbe, R. Auvergne, A. Gandini and B. Boutevin, *RSC Adv.*, 2015, **5**, 37742–37754.
4 Y.-L. Liu and W. Chuo, *Polym. Chem.*, 2013, **4**, 2194–2205.
5 T. N. Gevrek and A. Sanyal, *Eur. Polym. J.*, 2021, **153**, 110514.
6 C. E. Puerto Galvis, L. Y. Vargas Méndez and V. V. Kouznetsov, *Chem. Biol. Drug Des.*, 2013, **82**, 477–499.
7 T. A. Hill, S. G. Stewart, S. P. Ackland, J. Gilbert, B. Sauer, J. A. Sakoff and A. McCluskeya, *Bioorg. Med. Chem.*, 2007, **15**, 6126–6134.
8 L. Rulíšek, P. S. ˇ Ebek, Z. Havlas, R. Hrabal, P. C. ˇ Apek and A. Svatoš, *J. Org. Chem.*, 2005, **70**, 6295–6302.
9 L. Moed, T. A. Shwayder and M. W. Chang, *Arch. Dermatol.*, 2001, **137**, 1357–1360.
10 L. D. Bastin, M. Nigam, S. Martinus, J. E. Maloney, L. L. Benyack and B. Gainer, *Green Chem. Lett. Rev.*, 2019, **12**, 127–135.
11 R. J. Christie, R. Fleming, B. Bezabeh, R. Woods, S. Mao, J. Harper, A. Joseph, Q. Wang, Z. Q. Xu, H. Wu, C. Gao and N. Dimasi, *J. Control. Release*, 2015, **220**, 660–670.
12 M. Sortino, F. Garibotto, V. Cechinel Filho, M. Gupta, R. Enriz and S. Zacchino, *Bioorg. Med. Chem.*, 2011, **19**, 2823–2834.
13 K. I. Galkin and V. P. Ananikov, *Int. J. Mol. Sci.*, 2021, **22**, 11856.
14 J. Y. Wu, C. D. Kuo, C. Y. Chu, M. S. Chen, J. H. Lin, Y. J. Chen and H. F. Liao, *Molecules*, 2014, **19**, 6911–6928.
15 H. Özkan and Ş. Adem, *ChemistrySelect*, 2020, **5**, 5422–5428.
16 M. Abu-Laban, R. R. Kumal, J. Casey, J. Becca, D. Lamaster, C. N. Pacheco, D. G. Sykes, L. Jensen, L. H. Haber and D. J. Hayes, *J. Colloid Interface Sci.*, 2018, **526**, 312–321.
17 A. L. Widstrom and B. J. Lear, *Sci. Rep.*, 2019, **9**, 1–8.
18 S. Kotha and S. Banerjee, *RSC Adv.*, 2013, **3**, 7642–7666.
19 A. L. W. Demuynck, P. Levecque, A. Kidane, D. W. Gammon, E. Sickle, P. A. Jacobs, D. E. De Vos and B. F. Sels, *Adv. Synth. Catal.*, 2010, **352**, 3419–3430.
20 A. J. Thistlethwaite, D. B. Leeper, D. J. Moylan and R. E. Nerlinger, *Int. J. Radiat. Oncol. Biol. Phys.*, 1985, **11**, 1647–1652.
21 S. S. Cheng, Y. Shi, X. N. Ma, D. X. Xing, L. D. Liu, Y. Liu, Y. X. Zhao, Q. C. Sui and X. J. Tan, *J. Mol. Struct.*, 2016, **1115**, 228–240.
22 H. Chang, I. Bajaj, A. H. Motagamwala, A. Somasundaram, G. W.

Huber and C. T. Maravelias, *Green Chem.*, 2021, **23**, 3288.
23 H. Chang, A. H. Motagamwala, G. W. Huber and J. A. Dumesic, *Green Chem.*, 2019, **21**, 5532–5540.
24 E. B. Gilcher, H. Chang, M. Rebarchik, G. W. Huber and J. A. Dumesic, *ACS Catal.*, 2022, **12**, 10186–10198.
25 E. B. Gilcher, H. Chang, G. W. Huber and J. A. Dumesic, *Green Chem.*, 2022, **24**, 2146–2159.
26 H. Chang, E. B. Gilcher, G. W. Huber and J. A. Dumesic, *Green Chem.*, 2021, **23**, 4355–4364.
27 A. Maggiani, A. Tubul and P. Brun, *Chem. Commun.*, 1999, 2495–2496.
28 L. Cho and E. E. Klaus, *ASLE Trans.*, 2008, **24**, 119–124.
29 Z. Sheikh, M. N. Abdallah, A. A. Hanafi, S. Misbahuddin, H. Rashid and M. Glogauer, *Materials (Basel).*, 2015, **8**, 7913–7925.
30 K. Troev, G. Grancharov, R. Tsevi and A. Tsekova, *Polymer*, 2000, **41**, 7017–7022.
31 J. Kim and P. Sudbery, *J. Microbiol.*, 2011, **49**, 171–177.